Journal of Catalysis 340 (2016) 227–235

Contents lists available at ScienceDirect

Journal of Catalysis

journal homepage: www.elsevier.com/locate/jcat

On the stability and nature of adsorbed pentene in Brønsted acid zeolite H-ZSM-5 at 323 K

J. Hajek, J. Van der Mynsbrugge, K. De Wispelaere, P. Cnudde, L. Vanduyfhuys, M. Waroquier, V. Van Speybroeck *

Center for Molecular Modeling, Ghent University, Technologiepark 903, B-9052 Zwijnaarde, Belgium

ARTICLE INFO

Article history:
Received 12 February 2016
Revised 20 May 2016
Accepted 21 May 2016
Available online 14 June 2016

Keywords:
Molecular dynamics
Zeolites
Catalysis
Density functional theory
Adsorption

ABSTRACT

Adsorption of linear pentenes in H-ZSM-5 at 323 K is investigated using contemporary static and molecular dynamics methods. A physisorbed complex corresponding to free pentene, a π-complex and a chemisorbed species may occur. The chemisorbed species can be either a covalently bonded alkoxide or an ion pair, the so-called carbenium ion. Without finite temperature effects, the π-complex is systematically slightly more bound than the chemisorbed alkoxide complex, whereas molecular dynamics calculations at 323 K yield an almost equal stability of both species. The carbenium ion was not observed during simulations at 323 K. The transformation from the π-complex to the chemisorbed complex is activated by a free energy in the range of 33–42 kJ/mol. Our observations yield unprecedented insights into the stability of elusive intermediates in zeolite catalysis, for which experimental data are very hard to measure.

1. Introduction

Solid acids such as zeolites are widely applied in the chemical industry for conversion of hydrocarbons in reactions such as catalytic cracking, hydrocracking and alkylation [1–6]. These reactions involve alkanes and alkenes as reactants and products which interact with the zeolite and its Brønsted acid sites (BAS) [7]. The understanding of alkane adsorption on various zeolites has been the subject of numerous experimental studies, whereas comparatively little is known about adsorption of alkenes, due to their high reactivity even at low temperatures [8–10].

When an alkene adsorbs on a Brønsted acid zeolite, various adsorbed species may be distinguished as schematically indicated in Fig. 1 [11–14]. A first state corresponds to a free alkene in the cages of the zeolite, which undergoes only a weak van der Waals (vdW) interaction with the walls of the zeolite. This state is further referred to as the physisorbed state. A more bound state corresponds to the π-complex, where a specific non-bonded interaction between the π-electrons of the double bond and the Brønsted acid site occurs. Finally the π-complex may be protonated leading to the formation of a chemisorbed species [11–14]. The nature of the resulting intermediate is still debated. It has been proposed to be stabilized as a covalently bonded alkoxide or as an ion pair which is referred to as a free carbenium ion (Fig. 1) [11,12,15–17].

Alkene adsorption is very difficult to track experimentally as these hydrocarbons are highly reactive even at low temperatures. Solely based on experiment it is practically excluded to gain insight into the nature of the adsorbed complexes and intermediates, which can be very short-lived. For butenes some NMR and infrared based adsorption studies are available. The adsorption of butenes on H-ZSM-5 and mordenite was experimentally investigated by Domen et al. [12,13,17–19]. On H-ZSM-5, they observed that at sub-ambient temperatures a stable π-complex was formed and that double bond isomerization occurred already at 230 K [13,18,20]. A concerted mechanism was suggested to explain the rapid double bond isomerization despite the absence of a classical carbenium ion at these temperatures, as evidenced from isotope experiments [20–22]. Isotope experiments evidenced in addition the high mobility of alkenes already at sub-ambient temperatures [18,20]. Stepanov et al. studied the kinetics of the double-bond shift reaction, H/D exchange and ^{13}C scrambling for linear butenes on FER by means of ^{1}H, ^{2}H and ^{13}C MAS NMR for temperatures above 290 K and determined activation energies for the double bond shift and showed that carbenium ions are involved in the mechanism of double bond isomerization at higher temperatures [21,23].

Due to the lack of experimental data, theoretical studies are indispensable to obtain insight into the nature and stability of adsorbed species. Adsorption of alkanes has been studied extensively in the literature by various theoretical methods. A more complete literature overview may be found in some recent reviews

* Corresponding author.
E-mail address: veronique.vanspeybroeck@ugent.be (V. Van Speybroeck).

http://dx.doi.org/10.1016/j.jcat.2016.05.018
0021-9517/

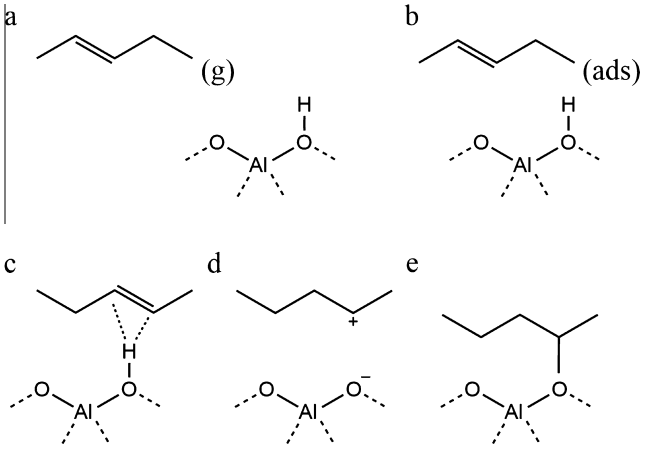

Fig. 1. Illustration of the different intermediates upon alkene (2-pentene) adsorption in the presence of a Brønsted acid site (BAS): (a) alkene in gas phase, (b) alkene physisorbed in the channels of the zeolite, (c) alkene π-complex, (d) chemisorbed carbenium ion and (e) chemisorbed alkoxide.

[24,25]. For alkenes much less information is available also from a theoretical point of view. In a series of papers by Sauer and co-workers various theoretical methods were used to study the adsorption behavior of C_4 species in H-FER [26,27]. The methods varied in the treatment of the molecular environment, the method to account for the long range dispersion interactions and the degree to which finite temperature effects were accounted for. All three factors are decisive to determine the relative stabilities of the π-complex, carbenium ions and alkoxide species. The stability of carbenium ions depends not only on the carbon skeleton, i.e. secondary, tertiary, cyclic, but also largely on the applied temperature. Higher temperatures may favor the existence of persistent carbenium ions. Nicholas and Haw concluded that stable carbenium ions could be observed by NMR provided that the neutral compound from which it originates has a proton affinity of 875 kJ mol^{-1} or larger [28]. However the topology of the material may also be very important as was shown by Fang et al. [29,30]. It was only very recently that the tert-butyl cation on H-ZSM-5 was identified by capturing this reaction intermediate with an ammonia molecule and by identifying the stable surface compounds by $^{1}H/^{13}C$ magic angle spinning NMR spectroscopy and density functional theory calculations [31]. The physisorption and chemisorption of alkenes beyond C_4 in a variety of zeolites (H-FAU, H-BEA, H-MOR, H-ZSM-5) were studied by Marin and co-workers using the QM-Pot methodology originally developed by Sauer and co-workers [14,32,33]. The method relies on a combination of a quantum mechanical approach on a smaller part of the system combined with an interatomic potential approach on the periodic structure. The QM-Pot methodology has proven to be very valuable in the time frame where periodic static calculations with more advanced functionals and dispersion interactions were unfeasible. Some earlier theoretical works also reported on the relative stabilities of alkenes, but this was done in the absence of dispersion interactions; however, also the importance of various rotational orientations of the adsorbed species was emphasized [11]. Indeed Göltl and co-workers stressed the role of finite temperature effects and mobility of adsorbed species in case of alkanes. For methane, ethane and propane in protonated chabazite at 300 K there was a substantial probability that the adsorbate desorbs from the acid site and moves freely in the pores of the zeolite, yielding adsorption enthalpies which are systematically smaller than the prediction at 0 K [34,35].

To the best of our knowledge no experimental data are available for alkene adsorption in H-ZSM-5 beyond C_4. Furthermore no fully periodic density functional theory calculations are available for the various adsorbed species of alkenes higher than C_4, neither from static calculations at 0 K nor from molecular dynamics calculations to account for finite temperature effects on the adsorption behavior. Such understanding is however crucial to optimize industrially important processes such as olefin cracking. These processes receive a lot of interest to selectively produce propene, by cracking less valuable C_4 through C_8 olefins [36–38]. Alkene cracking processes consist of a complex reaction network including isomerizations, oligomerizations, alkylations, hydride transfers and cracking reactions [3,7,39]. In any case, knowledge on the reaction intermediates is of utmost importance.

In this paper we present a complete study on the adsorption behavior of linear pentenes in H-ZSM-5, which is one of the most effective industrial catalysts for olefin production due to its optimal balance between conversion, selectivity and coke formation stability [40–42]. The applied methodology encompasses static periodic density functional theory calculations using contemporary density functionals and methods to account for the dispersion interactions, first principle molecular dynamics simulations at 323 K to account for the mobility of the adsorbates, and metadynamics simulations to sample the transformations among π-complex, alkoxide and carbenium ion and to deduce the corresponding free energy barriers. We took $T = 323$ K as finite temperature for all simulations. Inspection of the different adsorption studies in the literature learns that this temperature is representative to study the adsorption behavior at low temperatures. This complementary set of tools provides a comprehensive picture of the various adsorbed species in the absence of current relevant experimental data. Such insights into the relative stability of adsorbed species is of fundamental importance for our understanding of zeolite catalysis.

2. Computational methods

H-ZSM-5 was represented by a periodic model to fully account for the zeolite structure (Fig. S.1 of the SI). Static periodic Density Functional Theory (DFT) calculations were performed with the Vienna Ab Initio Simulation Package (VASP 5.3) [43–46]. Initial geometries were constructed with ZEOBUILDER [47]. The position of the Brønsted acid site (BAS) is the same as in earlier works of the authors [24,48] with a substitutional aluminum at the T12 position of the orthorhombic MFI unit cell and the charge compensating proton on O_{20}, resulting in a BAS at the intersection of the straight with sinusoidal channels (Fig. S.1). All structures were first optimized with a PBE functional using Grimme D3 dispersion corrections [49]. During the calculations the projector augmented approximation (PAW) [50,51] together with a plane wave kinetic energy cutoff of 600 eV was used and sampling of the Brillouin zone was restricted to the Γ-point. The convergence criterion for the electronic self-consistent field (SCF) problem was set to 10^{-5} eV. For all static periodic DFT calculations the unit cell was relaxed during the geometry optimizations. Afterward, the energy was refined with a variety of exchange correlation functionals and dispersion models encompassing revPBE-D3 with and without Becke Johnson damping (BJ) [52], revPBE with the non-local correlation functional vdW-DF of Dion [53], BEEF-vdW [54], and PBE with the new many body dispersion (MBD) scheme of Tkatchenko with conventional (MBD-vdW_H) and iterative Hirshfeld partitioning (MBD-vdW_HI) [55,56]. The thermal corrections were performed based on frequencies obtained with a partial Hessian approach including 8T atoms, the acid proton and the adsorbate. De Moor et al. [8] demonstrated that this type of procedure of using a partial Hessian is sufficient to determine accurate enthalpy and entropy differences. The nature of the local minima was

verified by a normal mode analysis showing that the partial Hessian matrix included only positive eigenmodes. We applied the partial Hessian vibrational analysis (PHVA) [55–57] as implemented in an in-house post-processing toolkit TAMkin [57].

Ab initio molecular dynamics (MD) simulations were performed with the CP2K software package [58] on the DFT level of theory by using the combined Gaussian Plane Wave basis sets approach [59,60]. The revPBE-D3 functional [61] together with the DZVP-GTH basis set and pseudopotentials were chosen [62]. This combination of exchange correlation functional and dispersion model was successfully used in earlier zeolite catalysis work [48,63,64]. Since ab initio molecular dynamics calculations performed on the complete zeolite model are computationally very expensive, more advanced methods using hybrid functionals or many body dispersion models are not feasible for simulations of considerable time length as emphasized here [65,66]. The cell parameters were determined from a preliminary NPT run on the empty zeolite unit cell at 323 K and 1 atm and are found to be $a = 20.14$ Å, $b = 20.33$ Å, $c = 13.56$ Å, $\alpha = 89.82°$, $\beta = 89.47°$, $\gamma = 90.15°$. Subsequent molecular dynamics and metadynamics (cf. infra) simulations on the various complexes were performed in the NVT ensemble at 323 K. The integration time step was set to 0.5 fs. The temperature was controlled by a chain of five Nosé-Hoover thermostats [67]. The MD simulations also allow the computation of finite-temperature adsorption enthalpies for the various π-complexes and alkoxides from ensemble averages of the internal energies over the MD trajectories from separate simulations on the complex, the empty zeolite and the adsorbate in gas phase. More details on the procedure and the influence of the length of the MD runs are given in the SI.

To accelerate sampling of the activated transition from the π-complex to the pentoxide and to explore the nature of the carbenium ion, a metadynamic (MTD) approach was employed [68,69]. This method has recently been applied successfully in various zeolite catalysis studies [63,70]. During an NVT MTD run with similar settings as for the MD simulations, Gaussian hills are added every 25 fs along two collective variables (CVs), described by coordination numbers (CN), which are able to describe the reaction coordinate for transformations between the various adsorbed species. The first CV is defined by CN(H—O)—CN(H—C_1) and describes the proton transfer from the zeolite to the pentene; the second CV is defined by CN(C_2—O_z) and describes the formation of the C—O bond between the resulting pentyl carbenium ion and the zeolite framework. C_1 and C_2 are the carbon atoms forming the double bond and visualized in Fig. 2 together with the definition of the collective variables. The metadynamics simulations yield a two-dimensional free energy surface in terms of the two collective variables. A 1D free energy profile is constructed by projecting the 2D free energy onto the minimum free energy path after which the free energy of activation may be computed [71]. More technical details of the simulations are taken up in the SI.

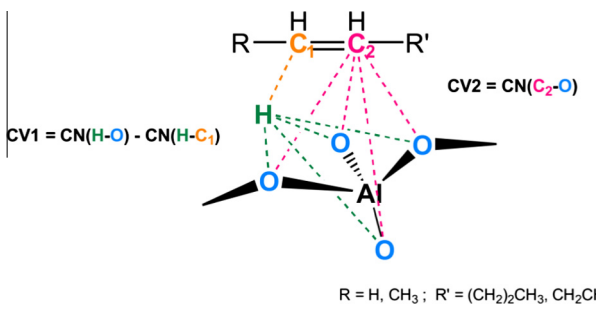

Fig. 2. Schematic visualization of the collective variables used for the various metadynamics simulations.

3. Results and discussion

To obtain insight into the mobility of the various adsorbed pentene species and the various plausible configurations, a series of ab initio MD runs were performed at 323 K on 1-pentene (π), 2-pentene (π), 2-pentoxide and 3-pentoxide complexes. As the potential energy surface (PES) contains a large number of local minima, we first performed a number of short MD runs of about 10 ps starting from an unbiased initial position corresponding to an orientation of the physisorbed pentene molecule in the center of the straight 10-membered ring cavity at about 4 Å from the acid site. We followed how the 2-pentene evolved during the initial stages of the simulation. In the Supporting Information we display some snapshots. The adsorbate that only interacts with the walls of the zeolite, quickly diffuses toward the acid site to form the π-complex. The 2-pentene molecule is preferentially positioned with the methyl end directed in the sinusoidal channel near the BAS and the longer ethyl tail in the straight cavity. These initial MD runs are then followed by more extensive production molecular dynamic runs of 100 ps starting from the optimal configuration obtained from the initial MD runs. The π-complex is characterized by the distance between the C=C double bond and the acid proton (H_z). The probability distribution of the shortest distance between one of the carbon atoms in the double bond and the acid proton during the simulation is plotted in Fig. 3. For both 1- and 2-pentene the shortest C—H_z distance is on average about 2 Å, indicating that the π—H interaction remains in place throughout the simulation. During the simulations at 323 K we did not observe the carbenium ion. For the alkoxides a similar analysis was done, yielding average C—O_z distances of about 1.6 Å, indicating that these complexes also remain stable during the simulation.

Besides geometrical features MD simulations also provide information about adsorption enthalpies. They are discussed further in the text where we investigated the influence of finite temperature effects on the adsorption process. First we report the 0 K results predicted by static calculations for the most visited structures.

In a next step, based on the probability distribution (Fig. 3) we determined adsorption positions corresponding to the most frequently visited structures during the MD runs and performed static calculations on these initial structures to get the optimized geometries. Subsequent frequency calculations lead finally to the adsorption enthalpies. For 1- and 2-pentene the energetically favorable configuration corresponds to the adsorbate positioned in the

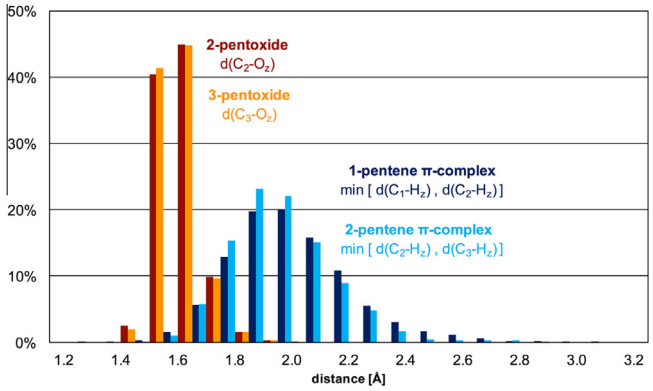

Fig. 3. Probability distributions of some critical distances in molecular dynamics simulations of π-complexes and alkoxides in H-ZSM-5 obtained over a 60 ps run. Min[d(C_1—H_z), d(C_2—H_z)] stands for the shortest C—H_z distance in 1-pentene π-complex [average 2.07 Å]; Min[d(C_2—H_z), d(C_3—H_z)] stands for the shortest distance in the 2-pentene π-complex [average: 2.04 Å]; d(C_2—O_z) is the C_2—O_z distance in 2-pentoxide complex [average: 1.62 Å]; and d(C_3—O_z) is the C_3—O_z distance in 3-pentoxide complex [average: 1.62 Å].

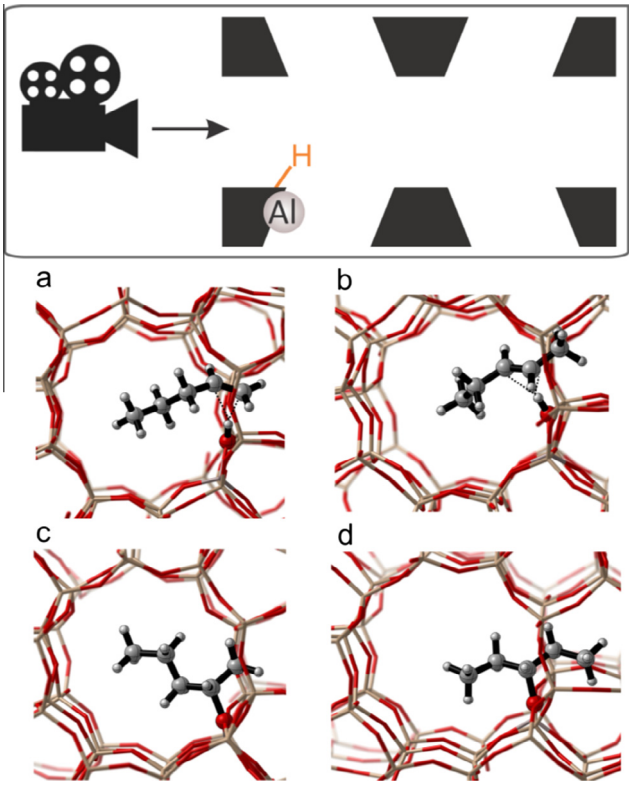

Fig. 4. MD snapshots of (a) 1-pentene π-complex, (b) 2-pentene π-complex, (c) chemisorbed 2-alkoxide and (d) chemisorbed 3-alkoxide in H-ZSM-5 at 323 K, seen in the direction of the straight channel (camera viewpoint). The snapshots correspond to geometries which are most frequently visited during MD runs of 100 ps at 323 K.

straight channel with its methyl tail oriented into the zigzag channel. The most plausible structures are visualized in Fig. 4. To ensure that the selected geometries for the static calculations do not substantially influence the obtained energetics, additional geometry optimizations were performed on a range of other geometries also generated from MD simulations. More details are taken up in Section 3.1 of the SI.

A decisive parameter for the energetics of the adsorbed species is the distance of the carbon skeleton with respect to the BAS. After optimization, the 1-pentene π-complex has a characteristic shortest C—H_z distance of about 1.9 Å. For 2-pentene π-complex this is about 2 Å. The pentoxide species are characterized by a C—O_z distance of about 1.6 Å. In order to check the influence of different functionals and dispersion models, we refined the energies using revPBE [53] and BEEF [54] functionals. Also some recently introduced dispersion models were tested such as the models of Tkatchenko et al. [55,56]. An overview of the adsorption enthalpies and free energies is given in Table 1 and Table S.3 of the SI. All applied levels of theories (LOT's) systematically predict the π-complexes more stable with respect to their chemisorbed counterparts by some 15–30 kJ/mol. The qualitative trends remain the same for all used levels of theory. The results show that the Becke–Johnson (BJ) damping function [52], revPBE-vdW-DF and BEEF-vdW levels of theory, even substantially enlarge the stability of the π-complexes compared with all other dispersion models, which indicates that these methods predict an overbinding of the adsorbed species (see Table 1).

Göltl and co-workers reached similar conclusions for the revPBE-vdW-DF method and an in-depth analysis was presented more recently by Göltl and Sautet [72].

To investigate also the influence of the level of theory on the geometry optimization and the derived relative stabilities of the π-complex and alkoxide structures, we also performed new geometry optimizations and frequency calculations for 2-pentene π-complex and 2-pentoxide using the BEEF-vdW functional [54]. Geometrical details of the structures with PBE-D3 and BEEF-vdW functionals are given in Table S.4. There are no essential features that are different, but the most crucial result is that the free energy and the adsorption enthalpy differences for the π-complex and chemisorbed complex are very similar to each other (Table 2) confirming our conclusions for the static calculations.

Our theoretical findings give qualitatively and quantitatively different results than the values of Nguyen et al. produced with the QM-Pot methodology [14]. Recently, also Rosch et al. found similar deviating behavior for alkanes between periodic DFT and QM-Pot results [73]. A proper analysis of possible ingredients lying at the basis of the observed differences, learns that the deviancies should not be ascribed to the QM-Pot methodology itself, but mainly to less favorable geometries of the adsorbed species and their positions in the cavity. In the case studied by Nguyen et al. [14], the double bond of 1- and 2-pentene was located at about 2.3 Å from the BAS, which is significantly larger than the distances predicted in this work. The PES around the adsorption site was explored in a 4T cluster embedded in the zeolite unit cell, and is by far not as accurate as the present calculations where the

Table 2
Free energy ΔG and enthalpy ΔH differences for configurations for the π-complex and chemisorbed complex in H-ZSM-5 at 323 K given in kJ/mol.

	BEEF-vdW //PBE D3		BEEF-vdW //BEEF-vdW	
	ΔG	ΔH	ΔG	ΔH
2-pentene (π) → 2-pentoxide	53.27	41.96	51.05	42.7

Table 1
Free energy ΔG and enthalpy ΔH differences for configurations for the π-complex and chemisorbed complex in H-ZSM-5 at 323 K. All energies in kJ/mol. Use of the standard notation "LOT-E"//"LOT-G" (LOT-E and LOT-G being the electronic levels of theory used for the energy and geometry optimizations, respectively).

	PBE-D3 //PBE-D3		revPBE-D3 //PBE-D3		revPBE-D3(BJ) //PBE D3		revPBE-vdW-DF //PBE D3		BEEF-vDW //PBE D3		PBE-MBD-vdW_H //PBE D3		PBE-MBD-vdW_HI //PBE D3	
	ΔG	ΔH	ΔG	ΔH	ΔG	ΔH	ΔG	ΔH	ΔG	ΔH	ΔG	ΔH	ΔG	ΔH
1-pentene (g) → 1-pentene (π)	−45.0	−103.2	−58.4	−116.6	−76.1	−134.3	−106.7	−164.9	−68.4	−126.6	−51.3	−109.5	−39.9	−98.1
2-pentene (g) → 2-pentene (π)	−52.7	−109.6	−73.3	−130.2	−90.7	−147.6	−112.4	−169.2	−71.1	−128.0	−58.6	−115.5	−44.7	−101.6
1-pentene (g) → 2-pentoxide	−17.5	−84.9	−40.1	−107.5	−60.3	−127.8	−69.2	−136.6	−29.4	−96.8	−30.6	−98.0	−15.0	−82.5
2-pentene (g) → 2-pentoxide	−4.1	−72.2	−28.7	−96.8	−47.4	−115.6	−58.2	−126.4	−17.8	−86.0	−17.2	−85.3	−1.4	−69.6
2-pentene (g) → 3-pentoxide	−3.0	−68.8	−21.3	−87.1	−39.8	−105.6	−52.9	−118.7	−14.1	−80.0	−19.9	−85.7	−2.8	−68.6
1-pentene (π) → 2-pentoxide	27.5	18.3	18.3	9.1	15.8	6.6	37.6	28.3	39.0	29.8	20.7	11.5	24.9	15.7
2-pentene (π) → 2-pentoxide	48.6	37.4	44.6	33.3	43.3	32.0	54.1	42.8	53.3	42.0	41.4	30.1	43.3	32.0
2-pentene (π) → 3-pentoxide	49.7	40.8	52.0	43.0	50.9	42.0	59.5	50.5	57.0	48.0	38.7	29.8	41.9	33.0

influence of the environment on the PES is intensively investigated in first-principles MD simulations of the periodic models. The geometries for 1- and 2-pentene reported in Ref. [14] differ by far from the configurations obtained in this work. On the other hand the geometrical parameters of the corresponding pentoxides found in the two studies are completely similar, so that the difference in stability between the physisorbed and chemisorbed complexes must be ascribed to the position of the physisorbed pentene to the BAS. This is an important statement as it reduces the discussion on the exothermic or endothermic character of the chemisorption process to the localization of the adsorbed pentene π-complex in the pores of the zeolite and more particularly the distance from the BAS.

In a next step, we assessed the influence of finite temperature effects on the adsorption enthalpies. The probability distributions for the distances of the various adsorbed species to the BAS, reveal an asymmetric behavior for the π-complexes toward higher C—H distances. For 1-pentene this is even more pronounced than for 2-pentene. The adsorption enthalpy of 1- and 2-pentene is strongly correlated with the C—H distance. The broad probability distribution for these two species clearly indicates that the average ensemble over the MD trajectories results in enthalpy of adsorption which corresponds to C—H distances larger than 2 Å. On the other hand, the static calculations only consider one point on the potential energy surface (that corresponds to the optimized geometry) and do not account for configurations with slightly larger distances as observed in the MD simulations. Indeed the dynamically averaged values for the adsorption enthalpies yield systematically lower adsorption enthalpies for the π-complexes and slightly larger values for the alkoxides. The adsorption enthalpies for the π-complexes are shifted to about 20 kJ/mol. Fig. 3 also reveals that the C—O_z distances in the pentoxides are more peaked around 1.6 Å with almost 80% probability yielding slightly more bound adsorption enthalpies from MD simulations. The adsorption enthalpies of pentoxides obtained as an ensemble average in the MD simulations are closer to the values obtained with static approaches. If finite temperature effects are taken into account the π-complexes are almost equally stable as the alkoxide species. A summarizing adsorption enthalpy diagram is given in Fig. 5. In good agreement with Ref. [11], the double bond position does not affect significantly the enthalpy of formation of the π-complex. Static calculations systematically overestimate the adsorption enthalpies for the π-complex, which is inherently related to the usage of optimized geometries, which are necessary to compute enthalpic and entropic contributions, but neglect the asymmetric probability distribution shown in Fig. 3 at finite temperatures.

Finally we also wanted to investigate the possible occurrence of carbenium ions in the transition path from π-complexes to alkoxides. Therefore we used metadynamics simulations which allow sampling the transition from the π-complex toward the chemisorbed species and exploring in how far the transformation

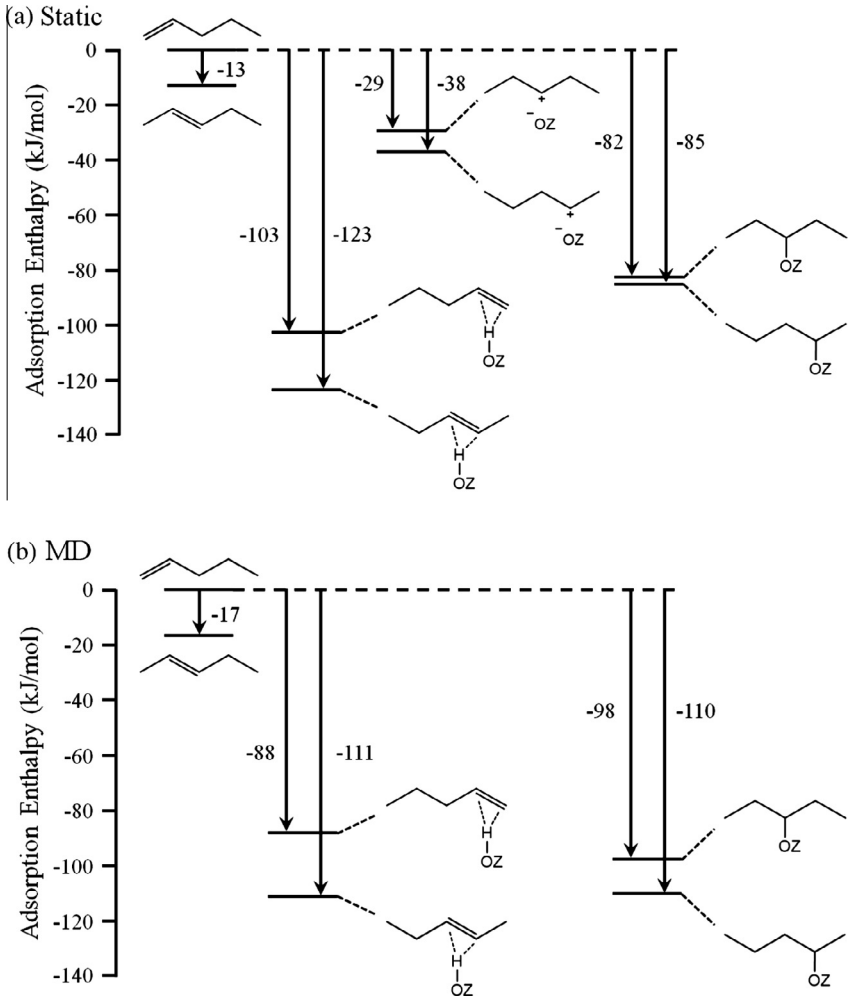

Fig. 5. Adsorption enthalpy diagrams at 323 K for the several pentene intermediates with reference to 1-pentene in gas phase and an empty H-ZSM-5 framework, obtained from (a) static calculations at the PBE-D3 level. (b) MD simulations at the revPBE-D3 level.

is activated. Those simulations yield detailed information on the nature of the chemisorbed species and the possible existence of a carbenium ion. In any case the carbenium ion was not observed during a regular MD run, nor was the transition from the π-complex toward the alkoxide seen, which points toward an activated transition.

The formation of 2-pentoxide from physisorbed 1-pentene and 2-pentene and that of 3-pentoxide from physisorbed 2-pentene were studied using metadynamics simulations with two collective variables to describe the reaction coordinate (cfr. Section 2). The resulting 2D free energy surfaces and 1D free energy profiles along the lowest free energy paths corresponding with the three reactions are displayed in Fig. 6. There clearly exists a metastable state between the pentene π-complex and the pentoxide, which could be characterized as a carbenium ion. This metastable state mainly represents a 2-pentyl carbenium ion in the two reactions leading to 2-pentoxide; however, rapid isomerization to a 3-pentyl carbenium ion was observed as well.

In a next step the trajectories obtained from the metadynamic simulations were examined to distinguish between the free energy minima of the various adsorbed species. All samples in which the collective variable, corresponding to the coordination number representative for the C—O_z bond formation with the zeolite framework, is smaller than a cutoff value are identified as alkoxides. A similar procedure was applied for the identification of the pentyl carbenium ions. The detailed procedure is described in the SI. The procedure shows that it is possible to identify various basins corresponding to alkoxides where the C—O distance is on average 1.6 Å and corresponding to carbenium ions where the average distance is 3 Å, which is significantly larger than the value (2.0 Å) obtained with MD simulations for the π-complex (Fig. 3). Here, some prudence should be taken into consideration as metadynamics does not generate an equilibrium ensemble and hence geometric parameters, given in MTD, are only indicative.

The 2D free energy surface is subsequently converted into a 1D free energy profile (by projection onto the minimum free energy path). For the three reactions under study the difference (CV2–CV1) of the two coordination numbers turned out to be a good estimate for the one-dimensional reaction coordinate. The three free energy profiles for pentoxide formation, displayed in Fig. 6, show

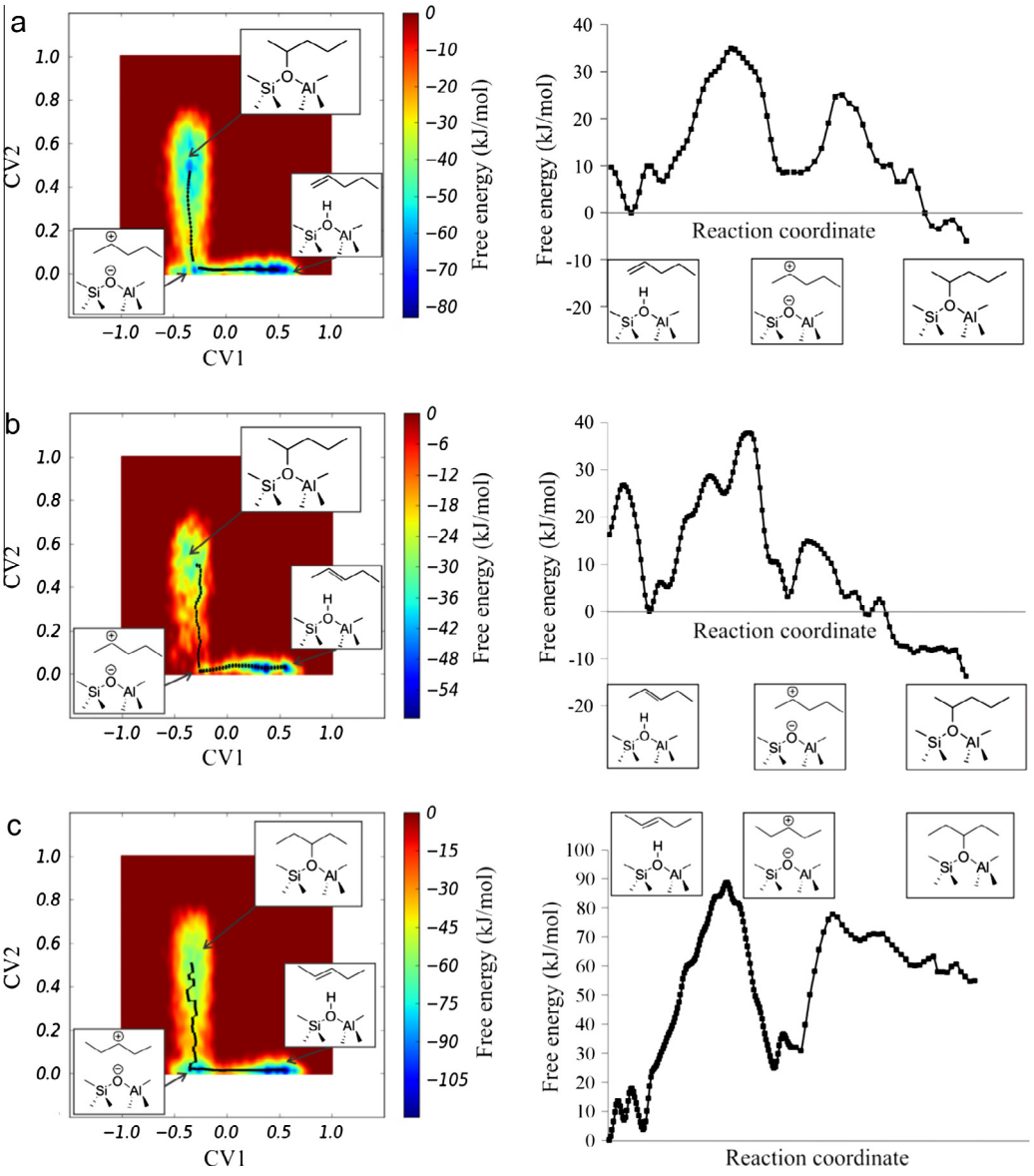

Fig. 6. Left: 2D free energy surface for the formation of 2-pentoxide from a 1-pentene π-complex (a) or 2-pentene π-complex (b) and for the formation of 3-pentoxide from a 2-pentene π-complex (c). The lowest free energy paths are displayed. A small well corresponding to the metastable carbenium ion can be observed in the bottom left corner. Right: corresponding 1D free energy profile along the lowest free energy path for the two reactions.

Table 3
Free energy barriers ($\Delta G^{\ddagger}$) and reaction free energies (ΔG_r) in kJ/mol at 323 K for the formation of a pentoxide from a pentene π-complex through a carbenium ion intermediate determined from MTD simulation in the NVT ensemble. LOT electronic energies: revPBE-D3/DZVP-GTH.

	$\Delta G^{\ddagger}$ (323 K) (kJ/mol)	ΔG_r (323 K) (kJ/mol)
1-pentene (π) → 2-pentyl carbenium	36.8	−2.3
2-pentyl carbenium → 2-pentoxide	20.3	−9.2
2-pentene (π) → 2-pentyl carbenium	38.2	+2.8
2-pentyl carbenium → 2-pentoxide	12.1	−15.2
2-pentene (π) → 3-pentyl carbenium	84.7	+22.9
3-pentyl carbenium → 3-pentoxide	54.6	+34.3

the carbenium ion as a metastable intermediate between the π-complex and the alkoxide. They also allow to determine some estimates of the free energy barriers ($\Delta G^{\ddagger}$) and reaction free energies (ΔG_r) between the various intermediate states following a procedure outlined in the SI. These values are listed in Table 3. It should be emphasized that free energies predicted by metadynamics are mainly qualitative, as they largely depend on the choice of the collective variables and other degrees of freedom. They give an indication of the minimum free energy path, but is not unique. Inclusion of other enhanced MD methods could be very complementary to MTD to compute enthalpy and Gibbs free energies. That work is planned in near future.

The observed free energy barriers for activation between the π-complex and the chemisorbed species vary considerably depending on the type of the chemisorption process. The formation of 2-pentoxides is likely to occur at these temperatures as the free energy of activation corresponds to about 36.8 kJ/mol for 1-pentene to 2-pentyl carbenium ion and 38.2 kJ/mol for 2-pentene to 2-pentyl carbenium ion. The formation of 3-pentoxide is less probable, a higher free energy of activation is found and the formed 3-pentoxide is less stable than the other alkoxides. This observation is systematically found for all methodologies used in this work, and is probably due to unfavorable steric interactions with the walls of the zeolite. MD simulations have revealed that by preference the shortest tail of the chemisorbed pentoxide is oriented in the zigzag channel. For a 2-pentoxide a methyl end enters the channel, while for a 3-pentoxide it is a propyl group (we refer to Fig. 4 for the visualization) encountering more interaction with the wall.

Apart from the formation of 3-pentoxide, the metadynamics simulations show that the alkoxide is only modestly more stable than the π-complex, which is in line with the earlier MD simulations.

Based on the metadynamics simulations, carbenium ions were observed and in a subsequent step these were also subjected to static periodic density functional theory calculations. Starting from configurations from the metadynamic simulations we could locate these highly elusive intermediates. The shortest C—O distance of the carbenium ion after this geometry optimization corresponds to 2.7 Å for the 2-pentyl carbenium ion and 3.4 Å for the 3-pentyl carbenium ion. The latter carbenium ion is further away from the BAS and is also about 10 kJ/mol less stable than the 2-pentyl carbenium ion. Based on the complementary set of simulations performed, we can now provide a full adsorption enthalpy diagram for all adsorbed species of 1-pentene and 2-pentene both from static and molecular dynamics simulations. This is visualized in Fig. 5 with all energy levels referred to the 1-pentene in the gas phase.

4. Conclusions

A complementary set of theoretical methods was used to fully characterize the adsorption behavior of pentene in the pores of H-ZSM-5. Four distinct states of the olefin have been investigated: (i) olefin adsorbed in the pores via dispersion forces, (ii) interactions of the C=C bond of pentene with the Brønsted acid sites in the pores (π-complex), (iii) the transient formation of a carbenium ion and (iv) the stable formation of an alkoxide. The free physisorbed pentene was not observed during a substantial time of a molecular dynamics run at 323 K, and instead a stable π-complex is rapidly formed, which does not transform toward alkoxides in a regular MD run but remains stable. This observation points toward an activated process to form stable chemisorbed species. The energies of π-complexes are very sensitive to the relative distance of the pentene molecule to the BAS. Adsorption enthalpies obtained from static calculations at 0 K are systematically larger than dynamically averaged values, since only the optimized structure of the π-complex at 0 K is taken into account. Thermal fluctuations on the relative distance of the complex with the BAS give a better representation of the dynamical adsorption process and give adsorption enthalpies which are on average 20–30 kJ/mol less stable compared to their static values. Static periodic calculations have the advantage that they allow to use a large variation of DFT functionals and dispersion models. Göltl et al. observed same features for the adsorption behavior of alkanes and proposed to dynamically weight statically obtained adsorption enthalpies [34]. Based on our observations this might indeed be a good practice for future adsorption studies. Overall the π-complex and alkoxides (except the 3-pentoxide) are almost equally stable. To sample also the transformation between stable π-complexes and alkoxides the metadynamics technique was used. During the transformation we observed the carbenium ion, which seems to be a highly elusive intermediate. Furthermore the transformation from a π-complex to the carbenium ion is activated with a free energy of activation in the range of 32–36 kJ/mol in the most favorable cases. Starting from geometries taken from the metadynamics simulations we also determined the enthalpies of the carbenium ion, with static density functional theory calculations. It was confirmed that carbenium ions are transient species lying higher in energy.

Overall the present data offer a new platform for understanding the adsorption steps of olefins on zeolites in a quantitative manner, which will in turn help to better understand the intrinsic role of the strength of the Brønsted acid sites and the role of the local environment (siting of acid sites, available pore space) for the adsorption processes in the future.

Acknowledgments

JVdM, KDW, JH, PC, MW and VVS acknowledge the Fund for Scientific Research – Flanders (FWO), the Research Board of Ghent University (BOF), BELSPO in the frame of IAP/7/05 and the fund for Scientific Research Flanders (FWO) for financial support. VVS and KDW acknowledge funding from the European Union's Horizon 2020 research and innovation programme (consolidator ERC grant agreement no. 647755 – DYNPOR (2015-2020)). The computational resources and services used in this work were provided by VSC (Flemish Supercomputer Center), funded by the Hercules foundation and the Flemish Government – department EWI. We

would like to thank Prof. Johannes Lercher and Dr. Maricruz Sanchez-Sanchez (Department of Chemistry and Catalysis Research Center, Technische Universität München) for fruitful discussions.

Appendix A. Supplementary material

Supplementary data associated with this article can be found, in the online version, at http://dx.doi.org/10.1016/j.jcat.2016.05.018.

References

[1] M. Guisnet, J.P. Gilson, Zeolites for Cleaner Technologies, Imperial College Press, London, 2002.
[2] A. Corma, Inorganic solid acids and their use in acid-catalyzed hydrocarbon reactions, Chem. Rev. 95 (1995) 559–614.
[3] J.S. Buchanan, J.G. Santiesteban, W.O. Haag, Mechanistic considerations in acid-catalyzed cracking of olefins, J. Catal. 158 (1996) 279–287.
[4] N. Rahimi, R. Karimzadeh, Catalytic cracking of hydrocarbons over modified ZSM-5 zeolites to produce light olefins: A review, Appl. Catal. A 398 (2011) 1–17.
[5] P.A. Jacobs, J.A. Martens, In Introduction to Zeolite Science and Practice, Elsevier, Amsterdam, 1991.
[6] W. Vermeiren, J.P. Gilson, Impact of zeolites on the petroleum and petrochemical industry, Top. Catal. 52 (2009) 1131–1161.
[7] Y.V. Kissin, Chemical mechanisms of catalytic cracking over solid acidic catalysts: alkanes and alkenes, Catal. Rev.-Sci. Eng. 43 (2001) 85–146.
[8] B.A. De Moor, M.F. Reyniers, O.C. Gobin, J.A. Lercher, G.B. Marin, Adsorption of C2–C8 n-alkanes in Zeolites, J. Phys. Chem. C 115 (2011) 1204–1219.
[9] F. Eder, J.A. Lercher, Alkane sorption in molecular sieves: the contribution of ordering, intermolecular interactions, and sorption on Brønsted acid sites, Zeolites 18 (1997) 75–81.
[10] F. Eder, M. Stockenhuber, J.A. Lercher, Brønsted acid site and pore controlled siting of alkane sorption in acidic molecular sieves, J. Phys. Chem. B 101 (1997) 5414–5419.
[11] A. Bhan, Y.V. Joshi, W.N. Delgass, K.T. Thomson, DFT investigation of alkoxide formation from olefins in H-ZSM-5, J. Phys. Chem. B 107 (2003) 10476–10487.
[12] H. Ishikawa, E. Yoda, J.N. Kondo, F. Wakabayashi, K. Domen, Stable dimerized alkoxy species of 2-methylpropene on mordenite zeolite studied by FT-IR, J. Phys. Chem. B 103 (1999) 5681–5686.
[13] J.N. Kondo, S. Liqun, F. Wakabayashi, K. Domen, IR study of adsorption and reaction of 1-butene on H-ZSM-5, Catal. Lett. 47 (1997) 129–133.
[14] C.M. Nguyen, B.A. De Moor, M.-F. Reyniers, G.B. Marin, Physisorption and chemisorption of linear alkenes in zeolites: a combined QM-Pot(MP2//B3LYP:GULP)-statistical thermodynamics study, J. Phys. Chem. C 115 (2011) 23831–23847.
[15] M. Boronat, P.M. Viruela, A. Corma, Reaction intermediates in acid catalysis by zeolites: prediction of the relative tendency to form alkoxides or carbocations as a function of hydrocarbon nature and active site structure, J. Am. Chem. Soc. 126 (2004) 3300–3309.
[16] V. Nieminen, M. Sierka, D.Y. Murzin, J. Sauer, Stabilities of C3–C5 alkoxide species inside H-FER zeolite: a hybrid QM/MM study, J. Catal. 231 (2005) 393–404.
[17] J.N. Kondo, F. Wakabayashi, K. Domen, IR study of adsorption of olefins on deuterated ZSM-5, J. Phys. Chem. B 102 (1998) 2259–2262.
[18] J.N. Kondo, K. Domen, F. Wakabayashi, Double bond migration of 1-butene without protonated intermediate on D-ZSM-5, Micropor. Mesopor. Mater. 21 (1998) 429–437.
[19] E. Yoda, J.N. Kondo, K. Domen, Detailed process of adsorption of alkanes and alkenes on zeolites, J. Phys. Chem. B 109 (2005) 1464–1472.
[20] J.N. Kondo, L. Shao, F. Wakabayashi, K. Domen, Double bond migration of an olefin without protonated species on H(D) form zeolites, J. Phys. Chem. B 101 (1997) 9314–9320.
[21] A.G. Stepanov, S.S. Arzumanov, M.V. Luzgin, H. Ernst, D. Freude, In situ monitoring of n-butene conversion on H-ferrierite by 1H, 2H, and 13C MAS NMR: kinetics of a double-bond-shift reaction, hydrogen exchange, and the 13C-label scrambling, J. Catal. 229 (2005) 243–251.
[22] M. Boronat, P. Viruela, A. Corma, Theoretical study of the mechanism of zeolite-catalyzed isomerization reactions of linear butenes, J. Phys. Chem. A 102 (1998) 982–989.
[23] A.G. Stepanov, M.V. Luzgin, S.S. Arzumanov, H. Ernst, D. Freude, N-butene conversion on H-ferrierite studied by 13C MAS NMR, J. Catal. 211 (2002) 165–172.
[24] V. Van Speybroeck, K. De Wispelaere, J. Van der Mynsbrugge, M. Vandichel, K. Hemelsoet, M. Waroquier, First principle chemical kinetics in zeolites: the methanol-to-olefin process as a case study, Chem. Soc. Rev. 43 (2014) 7326–7357.
[25] V. Van Speybroeck, K. Hemelsoet, L. Joos, M. Waroquier, R.G. Bell, C.R.A. Catlow, Advances in theory and their application within the field of zeolite chemistry, Chem. Soc. Rev. 44 (2015) 7044–7111.
[26] C. Tuma, T. Kerber, J. Sauer, The tert-Butyl Cation in H-Zeolites: deprotonation to isobutene and conversion into surface alkoxides, Angew. Chem.-Int. Ed. 49 (2010) 4678–4680.
[27] C. Tuma, J. Sauer, Protonated isobutene in zeolites: tert-butyl cation or alkoxide?, Angew Chem.-Int. Ed. 44 (2005) 4769–4771.
[28] J.B. Nicholas, J.F. Haw, The prediction of persistent carbenium ions in zeolites, J. Am. Chem. Soc. 120 (1998) 11804–11805.
[29] H. Fang, A. Zheng, J. Xu, S. Li, Y. Chu, L. Chen, F. Deng, Theoretical investigation of the effects of the zeolite framework on the stability of carbenium ions, J. Phys. Chem. C 115 (2011) 7429–7439.
[30] H. Fang, A. Zheng, S. Li, J. Xu, L. Chen, F. Deng, New insights into the effects of acid strength on the solid acid-catalyzed reaction: theoretical calculation study of olefinic hydrocarbon protonation reaction, J. Phys. Chem. C 114 (2010) 10254–10264.
[31] W.L. Dai, C.M. Wang, X.F. Yi, A.M. Zheng, L.D. Li, G.J. Wu, N.J. Guan, Z.K. Xie, M. Dyballa, M. Hunger, Identification of tert-Butyl Cations in Zeolite H-ZSM-5: evidence from NMR spectroscopy and DFT calculations, Angew. Chem.-Int. Ed. 54 (2015) 8783–8786.
[32] J. Sauer, M. Sierka, Combining quantum mechanics and interatomic potential functions in ab initio studies of extended systems, J. Comput. Chem. 21 (2000) 1470–1493.
[33] B.A. De Moor, M.F. Reyniers, G.B. Marin, Physisorption and chemisorption of alkanes and alkenes in H-FAU: a combined ab initio-statistical thermodynamics study, Phys. Chem. Chem. Phys. 11 (2009) 2939–2958.
[34] F. Goeltl, A. Grueneis, T. Bucko, J. Hafner, Van der Waals interactions between hydrocarbon molecules and zeolites: Periodic calculations at different levels of theory, from density functional theory to the random phase approximation and Moller-Plesset perturbation theory, J. Chem. Phys. 137 (2012) 114111.
[35] F. Goeltl, J. Hafner, Modelling the adsorption of short alkanes in protonated chabazite: the impact of dispersion forces and temperature, Micropor. Mesopor. Mater. 166 (2013) 176–184.
[36] J.Q. Chen, A. Bozzano, B. Glover, T. Fuglerud, S. Kvisle, Recent advancements in ethylene and propylene production using the UOP/Hydro MTO process, Catal. Today 106 (2005) 103–107.
[37] M.J. Tallman, C. Eng, Consider new catalytic routes for olefins production – innovative catalyst systems enable higher propylene make from liquid feedstocks, Hydrocarbon Process. 87 (2008) 95–101.
[38] T. von Aretin, S. Schallmoser, S. Standl, M. Tonigold, J.A. Lercher, O. Hinrichsen, Single-event kinetic model for 1-pentene cracking on ZSM-5, Ind. Eng. Chem. Res. 54 (2015) 11792–11803.
[39] J. Abbot, B.W. Wojciechowski, The Mechanism of catalytic cracking of normal-alkenes on ZSM-5 zeolite, Can. J. Chem. Eng. 63 (1985) 462–469.
[40] J.S. Buchanan, The chemistry of olefins production by ZSM-5 addition to catalytic cracking units, Catal. Today 55 (2000) 207–212.
[41] M.A. den Hollander, M. Wissink, M. Makkee, J.A. Moulijn, Gasoline conversion: reactivity towards cracking with equilibrated FCC and ZSM-5 catalysts, Appl. Catal. A-Gen. 223 (2002) 85–102.
[42] X.X. Zhu, S.L. Liu, Y.Q. Song, L.Y. Xu, Catalytic cracking of C4 alkenes to propene and ethene: influences of zeolites pore structures and Si/Al-2 ratios, Appl. Catal. A-Gen. 288 (2005) 134–142.
[43] G. Kresse, J. Furthmuller, Efficient iterative schemes for ab initio total-energy calculations using a plane-wave basis set, Phys. Rev. B 54 (1996) 11169–11186.
[44] G. Kresse, J. Furthmüller, Efficiency of ab-initio total energy calculations for metals and semiconductors using a plane-wave basis set, Comput. Mater. Sci. 6 (1996) 15.
[45] G. Kresse, J. Hafner, Ab initio molecular-dynamics for liquid-metals, Phys. Rev. B 47 (1993) 558–561.
[46] G. Kresse, J. Hafner, Ab initio molecular-dynamics simulation of the liquid-metal-amorphous-semiconductor transition in germanium, Phys. Rev. B 49 (1994) 14251.
[47] T. Verstraelen, V. Van Speybroeck, M. Waroquier, ZEOBUILDER: a GUI toolkit for the construction of complex molecular structures on the nanoscale with building blocks, J. Chem. Inf. Model. 48 (2008) 1530–1541.
[48] J. Van der Mynsbrugge, S.L.C. Moors, K. De Wispelaere, V. Van Speybroeck, Insight into the formation and reactivity of framework-bound methoxide species in H-ZSM-5 from static and dynamic molecular simulations, Chemcatchem 6 (2014) 1906–1918.
[49] S. Grimme, J. Antony, S. Ehrlich, H. Krieg, A consistent and accurate ab initio parametrization of density functional dispersion correction (DFT-D) for the 94 elements H-Pu, J. Chem. Phys. 132 (2010) 154104.
[50] P.E. Blöchl, Projector augmented-wave method, Phys. Rev. B 50 (1994) 17953.
[51] G. Kresse, D. Joubert, From ultrasoft pseudopotentials to the projector augmented-wave method, Phys. Rev. B 59 (1999) 1758–1775.
[52] S. Grimme, S. Ehrlich, L. Goerigk, Effect of the damping function in dispersion corrected density functional theory, J. Comput. Chem. 32 (2011) 1456–1465.
[53] M. Dion, H. Rydberg, E. Schroder, D.C. Langreth, B.I. Lundqvist, Van der Waals density functional for general geometries, Phys. Rev. Lett. 92 (2004) 246401.
[54] J. Wellendorff, K.T. Lundgaard, A. Mogelhoj, V. Petzold, D.D. Landis, J.K. Norskov, T. Bligaard, K.W. Jacobsen, Density functionals for surface science: exchange-correlation model development with Bayesian error estimation, Phys. Rev. B 85 (2012) 235149.
[55] A. Ambrosetti, A.M. Reilly, R.A. DiStasio Jr., A. Tkatchenko, Long-range correlation energy calculated from coupled atomic response functions, J. Chem. Phys. 140 (2014).

[56] T. Bučko, S. Lebègue, T. Gould, J. Ángyán, Many-body dispersion corrections for periodic systems: an efficient reciprocal space implementation, J. Phys.: Condens. Matter 28 (2016) 045201.
[57] A. Ghysels, T. Verstraelen, K. Hemelsoet, M. Waroquier, V. Van Speybroeck, TAMkin: a versatile package for vibrational analysis and chemical kinetics, J. Chem. Inf. Model. 50 (2010) 1736–1750.
[58] J. VandeVondele, M. Krack, F. Mohamed, M. Parrinello, T. Chassaing, J. Hutter, QUICKSTEP: fast and accurate density functional calculations using a mixed Gaussian and plane waves approach, Comput. Phys. Commun. 167 (2005) 103–128.
[59] G. Lippert, J. Hutter, M. Parrinello, The Gaussian and augmented-plane-wave density functional method for ab initio molecular dynamics simulations, Theoret. Chem. Acc. 103 (1999) 124–140.
[60] G. Lippert, J. Hutter, M. Parrinello, A hybrid Gaussian and plane wave density functional scheme, Mol. Phys. 92 (1997) 477–487.
[61] K. Yang, J.J. Zheng, Y. Zhao, D.G. Truhlar, Tests of the RPBE, revPBE, tau-HCTHhyb, omega B97X-D, and MOHLYP density functional approximations and 29 others against representative databases for diverse bond energies and barrier heights in catalysis, J. Chem. Phys. 132 (2010) 10.
[62] S. Goedecker, M. Teter, J. Hutter, Separable dual-space Gaussian pseudopotentials, Phys. Rev. B 54 (1996) 1703–1710.
[63] K. De Wispelaere, B. Ensing, A. Ghysels, E.J. Meijer, V. Van Speybroeck, Complex reaction environments and competing reaction mechanisms in zeolite catalysis: insights from advanced molecular dynamics, Chem.-Eur. J. 21 (2015) 9385–9396.
[64] S.L.C. Moors, K. De Wispelaere, J. Van der Mynsbrugge, M. Waroquier, V. Van Speybroeck, Molecular dynamics kinetic study on the zeolite-catalyzed benzene methylation in ZSM-5, ACS Catal. 3 (2013) 2556–2567.
[65] F. Goltl, J. Hafner, Alkane adsorption in Na-exchanged chabazite: the influence of dispersion forces, J. Chem. Phys. 134 (2011) 064102.
[66] L. Schimka, J. Harl, A. Stroppa, A. Grueneis, M. Marsman, F. Mittendorfer, G. Kresse, Accurate surface and adsorption energies from many-body perturbation theory, Nat. Mater. 9 (2010) 741–744.
[67] D. Frenkel, B. Smit, Understanding Molecular Simulation, Academic Press Inc, 2001.
[68] A. Laio, F.L. Gervasio, Metadynamics: a method to simulate rare events and reconstruct the free energy in biophysics, chemistry and material science, Rep. Prog. Phys. 71 (2008) 126601.
[69] A. Laio, M. Parrinello, Escaping free-energy minima, Proc. Natl. Acad. Sci. USA 99 (2002) 12562–12566.
[70] K. De Wispelaere, S. Bailleul, V. Van Speybroeck, Catal. Sci. Technol. (2016).
[71] B. Ensing, A. Laio, M. Parrinello, M.L. Klein, A recipe for the computation of the free energy barrier and the lowest free energy path of concerted reactions, J. Phys. Chem. B 109 (2005) 6676–6687.
[72] F. Goeltl, P. Sautet, Modeling the adsorption of short alkanes in the zeolite SSZ-13 using "van der Waals" DFT exchange correlation functionals: understanding the advantages and limitations of such functionals, J. Chem. Phys. 140 (2014) 154105.
[73] C.-C. Chiu, G.N. Vayssilov, A. Genest, A. Borgna, N. Roesch, Predicting adsorption enthalpies on silicalite and HZSM-5: a benchmark study on DFT strategies addressing dispersion interactions, J. Comput. Chem. 35 (2014) 809–819.